J Nanopart Res (2017) 19: 108
DOI 10.1007/s11051-017-3809-7

RESEARCH PAPER

Low concentrations of silver nanoparticles have a beneficial effect on wound healing in vitro

Nikola Ambrožová · Bohumil Zálešák · Jitka Ulrichová · Kateřina Čížková · Adéla Galandáková

Received: 26 May 2016 / Accepted: 1 March 2017 / Published online: 13 March 2017

Abstract Silver has been used in medical application for its antibacterial, antifungal, and anti-inflammatory effects. Silver nanoparticles (AgNPs) are currently in the spotlight. It was shown that their application can be useful in the management of wounds. Our study was conducted to determine whether AgNPs (average size 10.43 ± 4.74 nm) and ionic silver (Ag-I) could affect the wound healing in the in vitro model of normal human dermal fibroblasts (NHDF). We evaluated their effect on reactive oxygen species (ROS) generation and the expression of key transcription factors that coordinate the cellular response to oxidative stress [nuclear factor (erythroid-derived 2)-like 2 (Nrf2)] and inflammation [nuclear factor-κB (NF-κB)], expression of heme oxygenase-1 (HO-1), and interleukin-6 (IL-6) level. Isolated primary NHDF were scratched, heated (1 h; 42 °C), and cultured with AgNPs (0.25, 2.5, and 25 μg/ml) and Ag-I (0.025, 0.1, and 0.25 μg/ml) for 8 or 24 h. The ROS generation, Nrf2, NF-κB, and HO-1 protein expression and IL-6 protein level were then evaluated by standard methods. Non-cytotoxic concentrations of AgNPs (0.25 and 2.5 μg/ml) did not affect the ROS generation but activated the Nrf2/HO-1 pathway and decreased the NF-κB expression and IL-6 level in the in vitro wound healing model. AgNPs at concentrations of 0.25 and 2.5 μg/ml seem to be suitable for the intended application as a topical agent for wound healing, although the gene silencing technique, chemical inhibitors, and detailed time- and concentration-dependent experiments are needed for a comprehensive study of signaling pathway regulation. Further investigation is also necessary to exclude any possible adverse effects.

Keywords Silver nanoparticles · Normal human dermal fibroblasts · Wound healing · Nrf2 · HO-1 · NF-κB · Biomedicine · Nanomedicine

Abbreviations

AgNPs	Silver nanoparticles
Ag-I	Ionic silver
AP-1	Activating protein
COX-2	Cyclooxygenase-2
DMEM	Dulbecco's modified Eagle's medium
HO-1	Heme oxygenase-1
IL	Interleukin
NF-κB	Nuclear factor-kappa B
NHDF	Normal human dermal fibroblasts

N. Ambrožová · J. Ulrichová · A. Galandáková
Department of Medical Chemistry and Biochemistry, Faculty of Medicine and Dentistry, Palacký University, Olomouc, Czech Republic

N. Ambrožová · A. Galandáková (✉)
Institute of Molecular and Translational Medicine, Faculty of Medicine and Dentistry, Palacký University, Hněvotínská 3, 775 15 Olomouc, Czech Republic
e-mail: galandakova.a@seznam.cz

B. Zálešák
Department of Plastic and Aesthetic Surgery, University Hospital Olomouc, Olomouc, Czech Republic

K. Čížková
Department of Histology and Embryology, Faculty of Medicine and Dentistry, Palacký University, Olomouc, Czech Republic

Nrf2	Nuclear factor (erythroid-derived 2)-like 2
PBS	Phosphate-buffered saline
TNF-α	Tumor necrosis factor α

Introduction

Silver has been used in medical application since before the time of Christ for its antibacterial, antifungal, and anti-inflammatory effects, and even Hippocrates utilized silver preparations for managing ulcers and to stimulate wound healing (Alexander 2009). Due to increasing bacterial resistance against antibiotics, silver with its proven antibacterial effect, efficiency against multidrug-resistant organisms, and low systematic toxicity is being investigated. Silver compounds such as silver nitrate and sulfadiazine have been used in topical applications, but currently silver nanoparticles (AgNPs) are in the spotlight. It has been shown that the application of AgNPs onto skin wounds in both the burn and excisional mice model enhanced the efficiency of healing by accelerated re-epithelization and faster wound contraction and also improved the tensile properties of repaired skin by regulating collagen deposition and inhibiting its uncontrolled growth (Kwan et al. 2011). This beneficial effect was also observed in wounds without inflammation or infection, which confirms that AgNPs affected wound healing directly, probably through modulating cytokines in the cells. Liu et al. proved that AgNPs can increase the rate of wound closure through the promotion of proliferation and migration of keratinocytes and by driving the differentiation of fibroblasts into myofibroblasts. They showed that the proliferation of fibroblasts was suppressed, and thus, the creation of scars and keloids during wound healing was prevented (Liu et al. 2010). All of these outcomes suggest that AgNPs can be useful in the management of wounds. Nevertheless, there are some reports that indicated a potential risk to the environment and human health. Due to this, many studies are focused on the investigation of AgNP cytotoxicity to understand their effects on human health (Asha Rani et al. 2008; Carlson et al. 2008; Kang et al. 2012b; Kaur and Tikoo 2013; Piao et al. 2011a; Yen et al. 2009).

Oxidative stress has been suggested to be a cause of AgNP-mediated cell death (Carlson et al. 2008; Kang et al. 2012b; Piao et al. 2011a). Of the stress-related genes, the nuclear (erythroid-derived 2)-like 2 (Nrf2) transcription factor has been identified to be a key regulator of oxidative stress responses in several organs and tissues, including the skin. It has been shown that Nrf2 is involved in wound healing. An upregulated expression of Nrf2 was observed after skin injury (Pedersen et al. 2003), and its main function is the defense against ROS that are produced in large amounts in wounded and inflamed tissues and can cause hard cell damage (Keller et al. 2006). Recently, several reports suggested that exposure to AgNPs can affect Nrf2 expression, but their results are contradictory. Kang et al. showed that cells with low Nrf2 activity were relatively more sensitive to AgNP-induced toxicity than the cells with a stable expression of Nrf2. They observed that AgNP-treated Nrf2 knockdown renal epithelial cells exhibited a reduction in glutathione content and profoundly increased ROS production and DNA damage compared to the control cells. They further demonstrated that the Nrf2/GSH signaling pathway is activated in the response to AgNP-treated renal epithelial cells (Kang et al. 2012a). These results are in agreement with the report of Prasad et al., which observed the depletion of glutathione content and transcriptional activation of Nrf2 in HepG2 cells after exposure to AgNPs (Prasad et al. 2013). HO-1 is widely considered to be an important component of defense against oxidative stress. The expression of HO-1 is strongly dependent on activation through the Nrf2 pathway. Kang et al. found that the expression of HO-1 was not increased by AgNPs in Nrf2 knockdown ovarian cells, whereas HO-1 was highly elevated in the cells with a stable expression of Nrf2. They demonstrated that the Nrf2/HO-1 signaling pathway is activated in response to AgNP exposure in ovarian cells and thus plays a protective role in AgNP-induced DNA damage and consequent toxicity (Kang et al. 2012b). Similarly, Aueviriyavit et al. demonstrated the activation of the Nrf2/HO-1 signaling pathway in the cytoprotective response against AgNP exposure in Caco-2 cells and thus potentially also in intestinal cells (Aueviriyavit et al. 2014). In contrast, Piao et al. found a decreased transcriptional activation of Nrf2 and down-regulation of 8-oxoguanine DNA glycosylase 1 gene expression in AgNP-treated human Chang liver cells (Piao et al. 2011b).

Oxidative stress-induced redox signaling is known to involve the activation of redox-sensitive transcription factors. Nuclear factor-κB (NF-κB) is one such vital transcription factor regulated by the intracellular redox status, which is activated by ROS. The expression of

NF-κB is initiated in almost all cells as an innate immune reaction to invading microorganisms after wounds (Bonizzi and Karin 2004). Numerous chemokines, cytokines, enzymes, adhesion molecules, and inhibitors of apoptosis such as interleukin (IL)-1β, IL-6, IL-8, inducible NO synthase, and cyclooxygenase-2 (COX-2) are then produced (Ghosh et al. 1998). These molecules are necessary in the early protecting response against pathogens, but mistakes in their regulation can lead to many chronic diseases (Ben-Neriah and Karin 2011). Recently, some reports demonstrated that AgNPs activated the NF-κB signaling pathway in HepG2 cells (Prasad et al. 2013; Stępkowski et al. 2014), a mouse macrophage cell line (Nishanth et al. 2011), human T-lymfocyte cell line (Eom and Choi 2010), and human brain cancer cell line (Asha Rani et al. 2012). The activation of NF-κB by AgNPs results in the transcription of many genes involved in inflammatory response, such as COX-2, tumor necrosis factor α (TNF-α), IL-6, and IL-8 (Nishanth et al. 2011; Romoser et al. 2012).

Our study was conducted to determine whether AgNPs could affect wound healing in an in vitro model. For this purpose, we used normal human dermal fibroblasts (NHDF). We evaluated their effect on (i) ROS generation, (ii) expression of key transcription factors that coordinate the cellular response to oxidative stress (Nrf2) and/or inflammation (NF-κB), (iii) expression of HO-1, and (iv) IL-6 level. We compared the effect of AgNPs and ionic silver (Ag-I).

Materials and methods

Chemicals

AgNPs and ionic silver [$AgNO_3$ solution; (Ag-I)] were provided by NanoTrade s.r.o. (Czech Republic). Western Blotting Luminol Reagent, Nrf2 (C-20) rabbit polyclonal antibody, NF-κB p65 (C-20) rabbit polyclonal antibody, HO-1 (H-105) rabbit polyclonal antibody, actin (I-19) goat polyclonal antibody, horseradish peroxidase-conjugated goat anti-rabbit, and rabbit anti-goat antibodies were obtained from Santa Cruz Biotechnology (USA). Tris-glycine-SDS buffer and Tris-glycine buffer were obtained from BioTech (Czech Republic). PageRuler™ Prestained Protein Ladder and Pierce® bicinchoninic acid Protein Assay Reagent A and B were obtained from GeneTiCA (Czech Republic). Immuno-Blot™ polyvinylidene difluoride (PVDF) membrane, Solution 1 for Primary Antibodies, Solution 2 for Secondary Antibodies, and OmniPur® Acrylamide/Bis-acrylamide, 29:1, 40% Solution were bought from Merck Millipore (Germany). Human IL-6 Development Kit was obtained from PeproTech (USA). Dulbecco's modified Eagle's medium (DMEM), Ham-F12 Nutrient Mixture, heat-inactivated fetal calf serum, stabilized penicillin-streptomycin solution, amphotericin B, hydrocortisone, adenine, insulin, epidermal growth factor, 3,3′,5-triiod-L-thyronin, trypsin, ampicillin, crystal violet, hematoxylin, eosin B, dihydrofluorescein diacetate, KODAK BioMax light film, and all other chemicals were purchased from Sigma-Aldrich (USA).

Synthesis and characterization of AgNPs

AgNPs were provided by NanoTrade s.r.o. (Czech Republic). The particle was synthesized by chemically reducing silver nitrate ($AgNO_3$) with sodium borohydride ($NaBH_4$) as described in the Czech patent (CZ 304160 B6) (Kvítek et al. 2013). The accurate size, shape, state of dispersion, and zeta potential (in water and in serum-free DMEM) were described previously (Galandáková et al. 2016). The size distribution analysis showed that 50% of the AgNPs were between 5 and 40 nm in size, and their overall average size was 10.43 ± 4.74 nm. The zeta potential value was −22 mV (in water) and −14.6 mV (in serum-free DMEM). Spectrophotometrical analysis showed that the AgNPs diluted in water and serum-free DMEM have absorption maxima at 388 and 557 nm, respectively.

Isolation, cultivation, and characterization of cell culture

Normal human dermal fibroblasts (NHDF) were isolated from the skin of medically healthy donors, cultivated and characterized as described previously (Galandáková et al. 2016). Samples of skin were obtained from patients undergoing plastic surgery at the Department of Plastic and Aesthetic Surgery (University Hospital Olomouc). The tissue specimens were taken with the written agreement of the patient and the permission of the local Ethics Committee (Ethics Committee of the University Hospital and the Faculty of Medicine of Palacky University in Olomouc, reference number 41/09 from April 6, 2009). The isolated NHDF were characterized by their morphology and immunocytochemistry according

to their phenotype at the Department of Histology and Embryology, Faculty of Medicine and Dentistry, Palacký University Olomouc.

Treatment of cells

The effects of AgNPs and Ag-I on biological parameters, including toxicity, were evaluated previously (Galandáková et al. 2016). Based on these results, we used the non-toxic concentration of AgNPs (0.25, 2.5, and 25 μg/ml) and Ag-I (0.025, 0.1, and 0.25 μg/ml) for evaluating their effect on wound healing.

For the wound simulation, a slightly modified version of the standard method for studying wound healing was used (Liang et al. 2007). Briefly, NHDF were seeded onto Petri dishes (9.4 cm^2) at a density of 1×10^5 cells/cm^2. After incubation (24 h), the cells were scratched with a pipette tip (200 μl) and washed with phosphate-buffered saline (PBS), and then the serum-free DMEM was applied. After that, the cells were heated (1 h; 42 °C) to more closely approximate a real wound, where there is a temperature increase during inflammation. The cells were washed with PBS, and AgNPs (0.25, 2.5, 25 μg/ml) and Ag-I (0.025, 0.1, and 0.25 μg/ml) were then applied in serum-free DMEM and incubated for 8 and 24 h. Control cells were scratched, heated, and treated with a serum-free DMEM without AgNPs and Ag-I. After incubation, the media were collected and immediately frozen (−80 °C) for IL-6 determination. Cells were washed with PBS, harvested and ROS generation and the expression of Nrf2, HO-1, and NF-κB were evaluated.

Microscopical and morphometric analysis of cells

The images of scratched and heated cells with AgNPs and Ag-I, as well as scratched and heated, and non-scratched and non-heated control cells without AgNPs and Ag-I, were captured after 24 h of incubation using a Zeiss Axiom Axiovert 40 CFL microscope.

NHDF for morphometric analysis were seeded on cover slides. After adhesion, cells were cultured and treated in the same way as for phase contrast microscopy. Then, cells were fixed in cold methanol/acetone (1:1) for 15 min and stained by routine hematoxylin-eosin staining. All parameters were measured by ImageJ software (National Institute of Health, USA).

Scratch wound healing assay

NHDF were seeded onto a 24-well plate at a density of 1×10^5 cells/cm^2, scratched, and heated as was described above. Then, AgNPs (0.25, 2.5, 25 μg/ml) and Ag-I (0.025, 0.1, and 0.25 μg/ml) were applied in serum-free DMEM and incubated for 24 and 48 h. Negative control cells were scratched, heated, and treated with a serum-free DMEM without AgNPs and Ag-I while positive control cells were treated in DMEM with 10% of serum. After incubation, cells were washed with PBS, stained for 15 min by crystal violet (0.5% solution), and washed properly with water. The area of the scratch was accomplished by densitometric analysis using the software Centerline.

Evaluation of ROS generation

Intracellular ROS generation was monitored using a dihydrofluorescein diacetate assay, as described previously (Negre-Salvayre et al. 2002). Briefly, after treatment the cells were incubated with dihydrofluorescein diacetate (5 μM) for 15 min in the incubator at 37 °C. NHDF were then properly washed with PBS, scraped into 1 ml of ice-cold PBS, and sonicated on ice (20 cycles, intensity 5). The fluorescence was measured using a microplate spectrophotometer (INFINITE M200, Tecan, Switzerland) at specific excitation/emission wavelengths of 500/525 nm. The protein concentration was determined by Bradford assay.

HO-1, Nrf2, and NF-κB determination

The total protein expression of HO-1 and translocation of Nrf2 and NF-κB from the cytosol to the nucleus were investigated using Western immunoblot analysis. After incubation, NHDF were gently washed with PBS, scraped into ice-cold PBS, and centrifuged (4700 rpm, 5 min, 4 °C). The PBS was then removed, and the pellet was resuspended in lysis buffer A (10 mM HEPES, 10 mM KCl, 1.5 mM $MgCl_2$, 0.5 mM DTT, 0.1% *v/v* NP-40). After incubation (10 min, 4 °C), a cytosolic lysate was cleared by centrifugation (12,000 rpm, 10 min, 4 °C) and the pellet was resuspended in lysis buffer B (20 mM HEPES, 0.42 M NaCl, 0.2 mM EDTA, 1.5 mM $MgCl_2$, 0.5 mM DTT, 0.5 mM PMSF, 25% *v/v* glycerol). After incubation (30 min, 4 °C), the nuclear lysate was cleared by centrifugation (12,000 rpm, 20 min, 4 °C). The protein concentration was

determined by BCA assay. Proteins were separated by 10% SDS-polyacrylamide gel electrophoresis and transferred onto a PVDF membrane. Residual binding sites on the membrane were blocked using blocking buffer [5% non-fat dry milk (*w*/*v*) in 100 mM Tris-buffered saline (pH 7.5) with Tween 20 (0.05%, *v*/*v*)] for 2 h at room temperature. The membrane was then incubated (4 °C, overnight) with the polyclonal primary antibody (rabbit anti-HO-1, rabbit anti-Nrf2, rabbit anti-NF-κB, and goat anti-actin) and then with an appropriate secondary horseradish peroxidase conjugated antibody (goat anti-rabbit and rabbit anti-goat) for 2 h at room temperature. The protein expression was detected by chemiluminescence using Western Blotting Luminol Reagent and autoradiography using a KODAK BioMax light film. The quantification of proteins was accomplished by densitometric analysis using the software ElfoMan 2.6.

Interleukin-6 determination

The amount of IL-6 was determined using a specific immunoassay Human IL-6 ELISA Development Kit (PeproTech, USA) according to the manufacturer's instructions. All samples were measured in duplicate. The detection limit was 24 pg/ml.

Statistical analysis

The series of experiments were performed in at least three independent experiments. The data are expressed as means + SD. Statistical analysis was performed using Student's *t* test. Statistical significance was determined at $p = 0.05$ (*), $p = 0.01$ (**), or $p = 0.001$ (***).

Results

Effect of AgNPs and Ag-I on cell morphology

The scratched and heated cells exposed to AgNPs (Fig. 1c–e) and Ag-I (Fig. 2c–e) and controls [non-scratched and non-heated cells (Figs. 1a and 2a) and scratched and heated cells (Figs. 1b and 2b)] without AgNPs and Ag-I showed the characteristic morphology for NHDF, except for the cells treated with AgNPs at a concentration of 25 μg/ml (Fig. 1e). It seems that this concentration of AgNPs was too high, because it overlay all the cells and the cell morphology was difficult to evaluate. Nevertheless, the only effect that can be possible to observe on these images is probably the increase of matrix phase mobility. The distance between scratched cells (Figs. 1b–d and 2b–e) is greater than that of original cells [non-scratched and non-heated NHDF without AgNPs and Ag-I (Figs. 1a and 2a)]. Due to this, cell morphology was evaluated during our experiments by nucleoplasmic ratio and no significant differences were observed in the length/width ratio compared to non-scratched and non-heated control (Table 1). The nucleoplasmic ratio moderately significantly decreased after the application of AgNPs (0.25 μg/ml) for 24 h compared to non-heated and non-scratched control while it significantly increased after the application of Ag-I (0.1 μg/ml).

Effect of AgNPs and Ag-I on the wound

For verifying that AgNPs and Ag-I may have an impact on wound healing, we provided a scratch assay. Our results showed that the wound area diminished after the application of AgNPs (0.25, 2.5, and 25 μg/ml) for both time intervals compared to the scratched and heated negative control cells but a significant decrease was found at concentrations 0.25 and 2.5 μg/ml after 48 h (Fig. 3a). The effect of Ag-I on the wound area is contrary as shown in Fig. 3b. The wound area increased after the application of Ag-I (0.025, 0.1, and 0.25 μg/ml) for both time intervals compared to the scratched and heated negative control cells, but a significant increase was found only at concentration 0.25 μg/ml after 48 h.

Effect of AgNPs and Ag-I on ROS generation

Despite the previous study (Galandáková et al. 2016) showing that AgNPs (0.25, 2.5, and 25 μg/ml) and Ag-I (0.025, 0.1, and 0.25 μg/ml) were non-toxic, we checked whether they affect ROS generation in non-scratched and non-heated NHDF. Our results showed that the treatment of non-scratched and non-heated NHDF with AgNPs and Ag-I (8 and 24 h) did not induce ROS generation compared to untreated non-scratched and non-heated NHDF (data not shown).

The effect of AgNPs on ROS generation in scratched and heated NHDF is shown in Fig. 4a. The application of AgNPs (0.25, 2.5 μg/ml) did not affect ROS generation, but the concentration of 25 μg/ml after 24 h significantly decreased the ROS level compared to the scratched and heated control. As shown in Fig. 4b, the

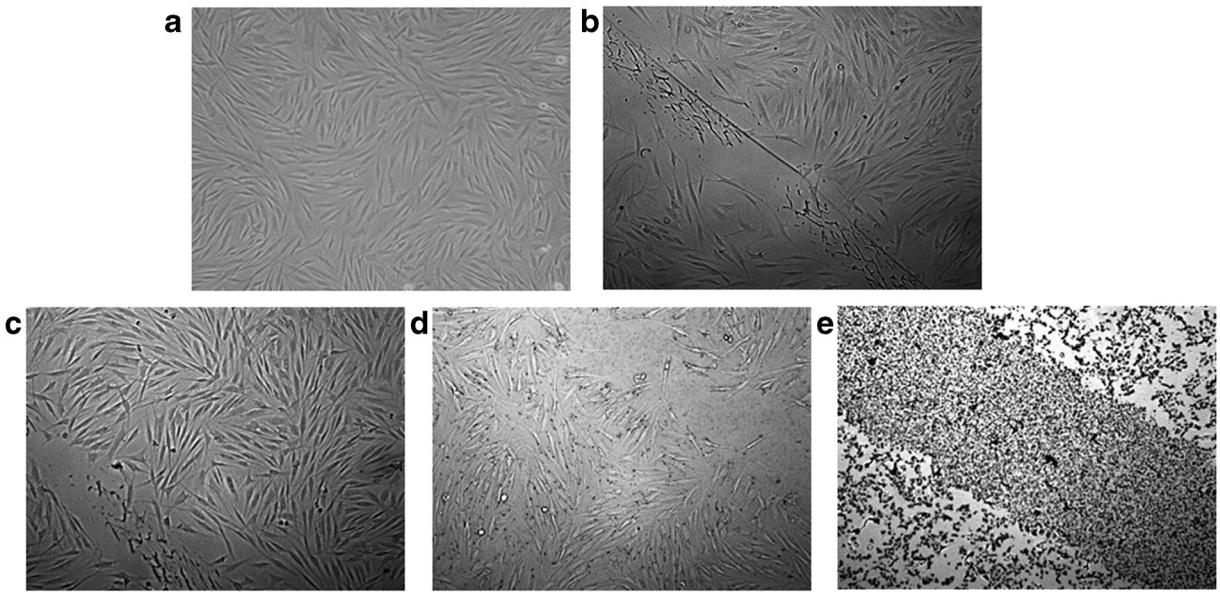

Fig. 1 NHDF treated with AgNPs for 24 h. The images of **a** non-scratched and non-heated cells without AgNPs, **b** scratched and heated cells without AgNPs, and scratched and heated cells with AgNPs **c** 0.25 μg/ml, **d** 2.5 μg/ml, and **e** 25 μg/ml were captured with a Zeiss Axiom Axiovert 40 CFL microscope. Magnification ×100

application of Ag-I at concentrations of 0.025 μg/ml for 24 h, 0.1 μg/ml for 8 and 24 h, and 0.25 μg/ml for 8 h significantly increased the ROS level compared to the scratched and heated control.

Effect of AgNPs and Ag-I on nuclear Nrf2 expression

Western blot analysis showed a significant increase in nuclear Nrf2 level with AgNPs (0.25 and 2.5 μg/ml) after

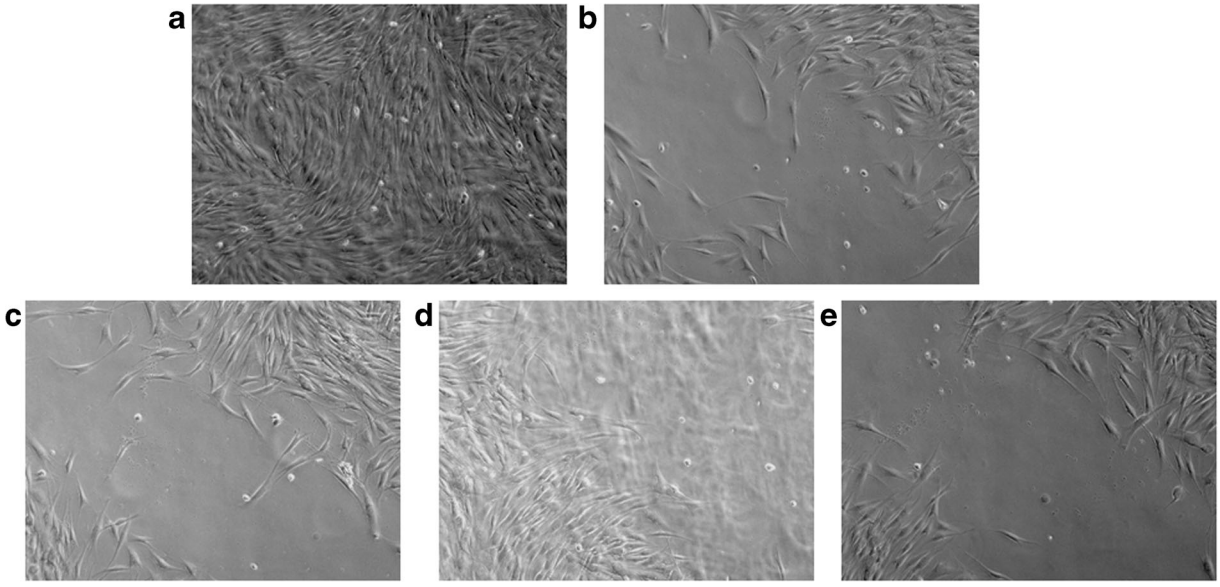

Fig. 2 NHDF treated with Ag-I for 24 h. The images of **a** non-scratched and non-heated cells without Ag-I, **b** scratched and heated cells without Ag-I, and scratched and heated cells with Ag-I **c** 0.025 μg/ml, **d** 0.1 μg/ml, and **e** 0.25 μg/ml were captured with a Zeiss Axiom Axiovert 40 CFL microscope. Magnification ×100

Table 1 Morphometric analysis

Treatment (μg/ml)	Scratching and heating	Length (μm)	Width (μm)	L/W index	N/C ratio
None—control	No	134.56 ± 30.73	18.03 ± 4.32	8.00 ± 2.94	0.17 ± 0.05
None—control	Yes	149.69 ± 25.27	17.21 ± 4.77	9.18 ± 2.53	0.15 ± 0.08
AgNPs 0.25	Yes	131.51 ± 21.65	15.17 ± 2.62	8.87 ± 1.76	0.14 ± 0.04*
AgNPs 2.5	Yes	111.63 ± 20.45	15.02 ± 4.46	7.98 ± 2.47	0.15 ± 0.04
AgNPs 25	Yes	123.68 ± 19.44	17.41 ± 5.14	7.73 ± 2.98	0.15 ± 0.05
Ag-I 0.025	Yes	121.13 ± 26.05	14.75 ± 3.46	8.54 ± 2.35	0.18 ± 0.05
Ag-I 0.1	Yes	128.08 ± 27.87	15.74 ± 4.18	8.64 ± 2.78	0.22 ± 0.06**
Ag-I 0.25	Yes	132.76 ± 23.84	17.11 ± 3.09	7.99 ± 2.09	0.18 ± 0.04

After 24 h treatment, NHDF were fixed in cold methanol/acetone (1:1) for 15 min and then stained by routine hematoxylin-eosin staining. All parameters were measured by ImageJ software. Data are expressed as means ± SD

L/W index length/width, *N/C ratio* nucleoplasmic ratio (nuclear area against total cell area)

*$p \leq 0.05$; **$p \leq 0.01$, significantly different from non-scratched and non-heated control cells

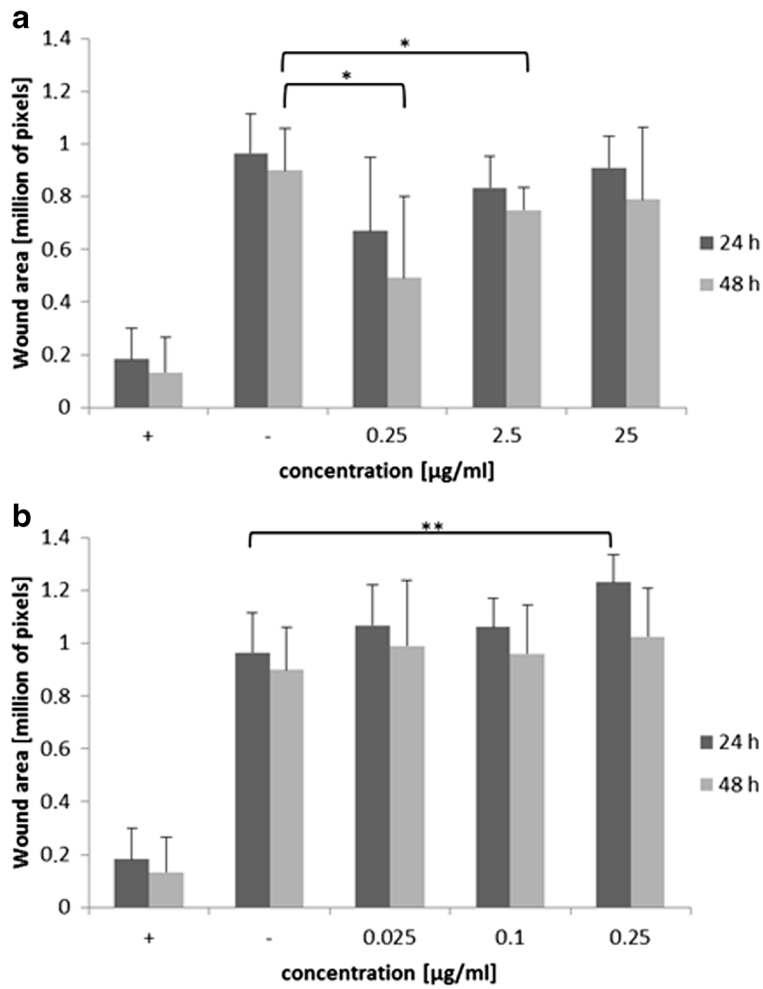

Fig. 3 Effects of AgNPs and Ag-I on the wound. Scratched and heated cells were treated with **a** AgNPs (0.25, 2.5, and 25 μg/ml) and **b** Ag-I (0.025, 0.1, and 0.25 μg/ml) for 24 and 48 h. Scratched and heated controls were treated with medium without AgNPs or Ag-I with serum (positive control (+)) or without serum (negative control (−)) under the same conditions. The wound area was determined by densitometric analysis using the software Centerline. Data are representative of four independent experiments expressed as means + SD. *$p \leq 0.05$ and **$p \leq 0.01$ are significantly different from negative control cells

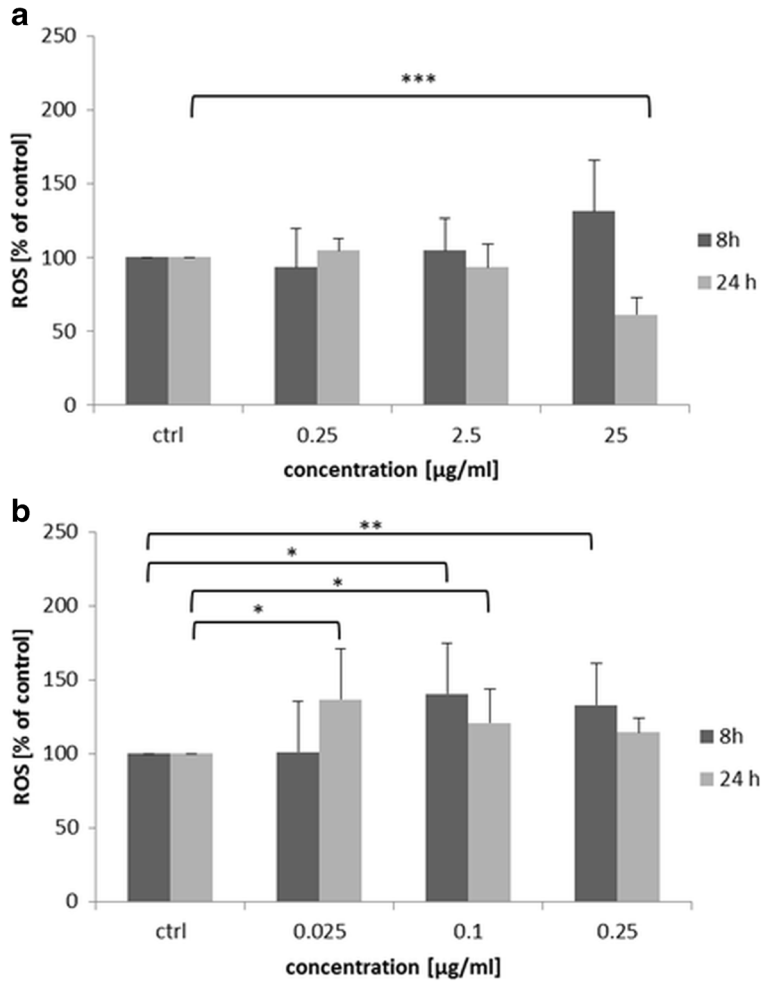

Fig. 4 Effects of AgNPs and Ag-I on ROS generation in NHDF. Scratched and heated cells were treated with **a** AgNPs (0.25, 2.5, and 25 μg/ml) and **b** Ag-I (0.025, 0.1, and 0.25 μg/ml) for 8 and 24 h. Scratched and heated controls were treated with medium without AgNPs or Ag-I under the same conditions. Data are representative of three independent experiments expressed as means + SD. *$p \leq 0.05$, **$p \leq 0.01$, and ***$p \leq 0.001$ are significantly different from scratched and heated cells

8 h and a significant decrease at the same concentrations of AgNPs after 24 h compared to the scratched and heated control cells. Further, AgNPs at 25 μg/ml decreased the nuclear Nrf2 level compared to the scratched and heated control for both time intervals (Fig. 5a, c). The effect of Ag-I on nuclear Nrf2 level is shown in Fig. 5b, d. Nuclear Nrf2 level was significantly increased after the application of Ag-I at a concentration of 0.1 μg/ml after 8 h and 0.025 μg/ml after 24 h compared to the scratched and heated control cells. The application of Ag-I at the highest concentration of 0.25 μg/ml significantly decreased the nuclear Nrf2 level after 24 h compared to the scratched and heated control cells.

Effect of AgNPs and Ag-I on HO-1 expression

AgNPs and Ag-I increased HO-1 expression as determined by western blot analysis. AgNPs (Fig. 6a, c) exhibited a concentration- and time-dependent increase in HO-1 level compared to the scratched and heated control cells after 8 and 24 h, even though the significant increase in HO-1 level was observed after only 8 h. The effect of Ag-I on HO-1 expression was lower than that of AgNPs (Fig. 6b, d). Ag-I produced a concentration-dependent increase in HO-1 level after 24 h, but its level did not change after 8 h.

Effect of AgNPs and Ag-I on nuclear NF-κB expression

The nuclear NF-κB level significantly increased after the application of AgNPs (0.25 μg/ml) for 8 h, but its level significantly decreased after a 24-h application of 0.25 and 2.5 μg/ml compared to the scratched and heated control cells (Fig. 7a, c). The highest concentration of AgNPs (25 μg/ml) had no effect on nuclear NF-κB level for both time

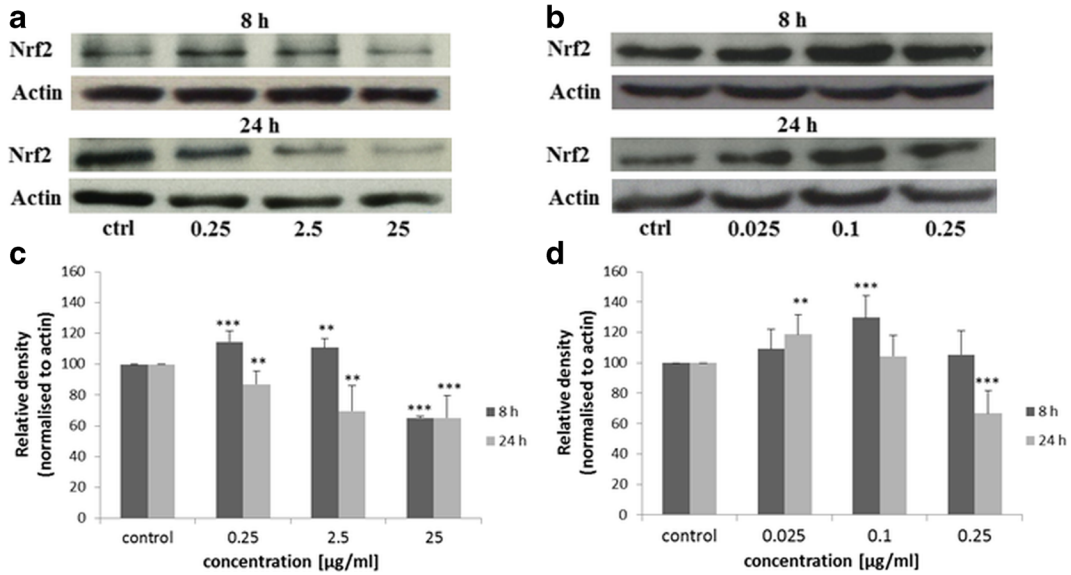

Fig. 5 Effects of AgNPs and Ag-I on nuclear Nrf2 level in NHDF. Scratched and heated cells were treated with AgNPs (0.25, 2.5, and 25 μg/ml) and Ag-I (0.025, 0.1, and 0.25 μg/ml) for 8 and 24 h. Scratched and heated controls were treated with medium without AgNPs or Ag-I under the same conditions. **a**, **b** Effects on protein expression. **c**, **d** Quantification of proteins performed by densitometric analysis using the software ElfoMan 2.6. Data are representative of three independent experiments expressed as means + SD. $^{**}p \leq 0.01$ and $^{***}p \leq 0.001$ are significantly different from scratched and heated cells

intervals. The effect of Ag-I on nuclear NF-κB level is shown in Fig. 7b, d. Ag-I (0.1 μg/ml) significantly increased the nuclear NF-κB level after 8 h, while the concentrations of 0.025 and 0.25 μg/ml significantly decreased its level after 24 h compared to the scratched and heated control cells.

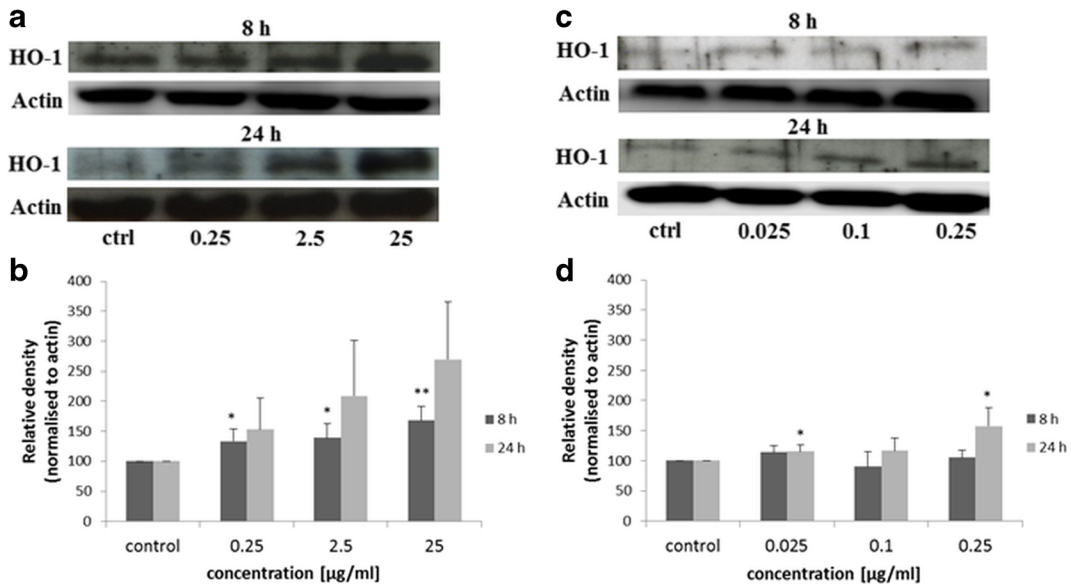

Fig. 6 Effects of AgNPs and Ag-I on HO-1 level in NHDF. Scratched and heated cells were treated with AgNPs (0.25, 2.5, and 25 μg/ml) and Ag-I (0.025, 0.1, and 0.25 μg/ml) for 8 and 24 h. Scratched and heated controls were treated with medium without AgNPs or Ag-I under the same conditions. **a**, **b** Effects on protein expression. **c**, **d** Quantification of proteins performed by densitometric analysis using the software ElfoMan 2.6. Data are representative of three independent experiments expressed as means + SD. $^{*}p \leq 0.05$ and $^{**}p \leq 0.01$ are significantly different from scratched and heated cells

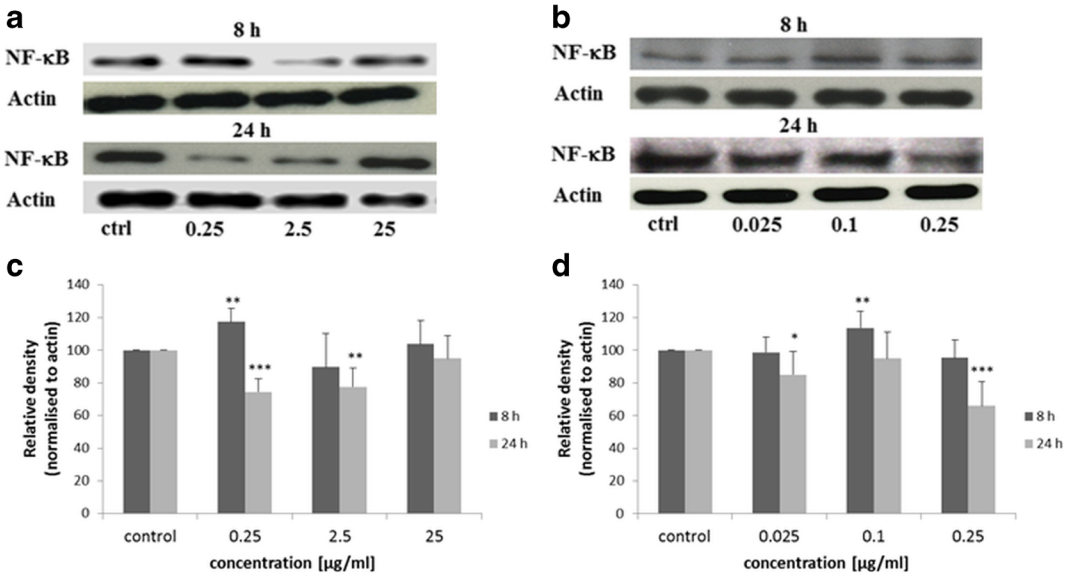

Fig. 7 Effects of AgNPs and Ag-I on NF-κB level in NHDF. Scratched and heated cells were treated with AgNPs (0.25, 2.5, and 25 μg/ml) and Ag-I (0.025, 0.1, and 0.25 μg/ml) for 8 and 24 h. Scratched and heated controls were treated with medium without AgNPs or Ag-I under the same conditions. **a**, **b** Effects on protein expression. **c**, **d** Quantification of proteins performed by densitometric analysis using the software ElfoMan 2.6. Data are representative of three independent experiments expressed as means + SD. $*p \leq 0.05$, $**p \leq 0.01$, and $***p \leq 0.001$ are significantly different from scratched and heated cells

Effect of AgNPs and Ag-I on IL-6 level

Medium harvested from NHDF exposed to AgNPs (0.25, 2.5, and 25 μg/ml) and Ag-I (0.025, 0.1, and 0.25 μg/ml) after 8 and 24 h was used for the determination of IL-6 level by ELISA assay. The result showed that AgNPs (0.25 and 2.5 μg/ml) decreased the IL-6 level after 24 h, while the highest concentration (25 μg/ml) increased the IL-6 level after 8 h compared to the scratched and heated control cells (Fig. 8a). Ag-I was not found to have any effect on IL-6 level (Fig. 8b).

Discussion

AgNPs have been commonly used in recent years, especially for their antibacterial and anti-inflammatory effects. It was shown that AgNPs have the potential to promote wound healing through facilitated anti-inflammatory action. Further, they could contribute positively to the process of re-epithelization, enhance the differentiation of fibroblasts to myofibroblasts, and promote the proliferation and migration of keratinocytes, thus increasing the rate of wound closure. Moreover, AgNPs improved the tensile properties of the repaired skin, with a close resemblance to normal skin (Kwan et al. 2011; Liu et al. 2010; Tian et al. 2007). This study aimed to investigate whether the non-toxic concentration of AgNPs could support wound healing through the modulation of key transcription factors that coordinate the cellular response to oxidative stress (Nrf2) and inflammation (NF-κB) in normal human dermal fibroblasts (NHDF). The effects of AgNPs were compared to ionic silver (Ag-I).

AgNPs are already being used in wound dressings and antibacterial clothing, but the dermal exposure form is a potential absorption route of AgNPs. A change in cell morphology is the first effect that can be seen in cells after exposure to nanoparticles. Due to this, cell morphology was evaluated during our experiments by nucleoplasmic ratio. NHDF exposed to AgNPs (0.25, 2.5, and 25 μg/ml) of 10.43 ± 4.74 nm size and Ag-I (0.025, 0.1, and 0.25 μg/ml) for 24 h did not stimulate almost any changes compared to the untreated control cells (Table 1). Kaur et al. observed a swelling of cells and cytoplasmic membrane damage in the A431cell line after a 24-h treatment with AgNPs (50 and 100 μg/ml) of diameter 30–50 nm (Kaur and Tikoo 2013). Lee et al. described the marks of cell death (shrinking, many floating cells, decrease in proliferation) in mouse embryonal fibroblasts exposed to AgNPs (30 μg/ml) of 26.0 ± 7.6 nm size for 24 h (Lee et al. 2014). Less

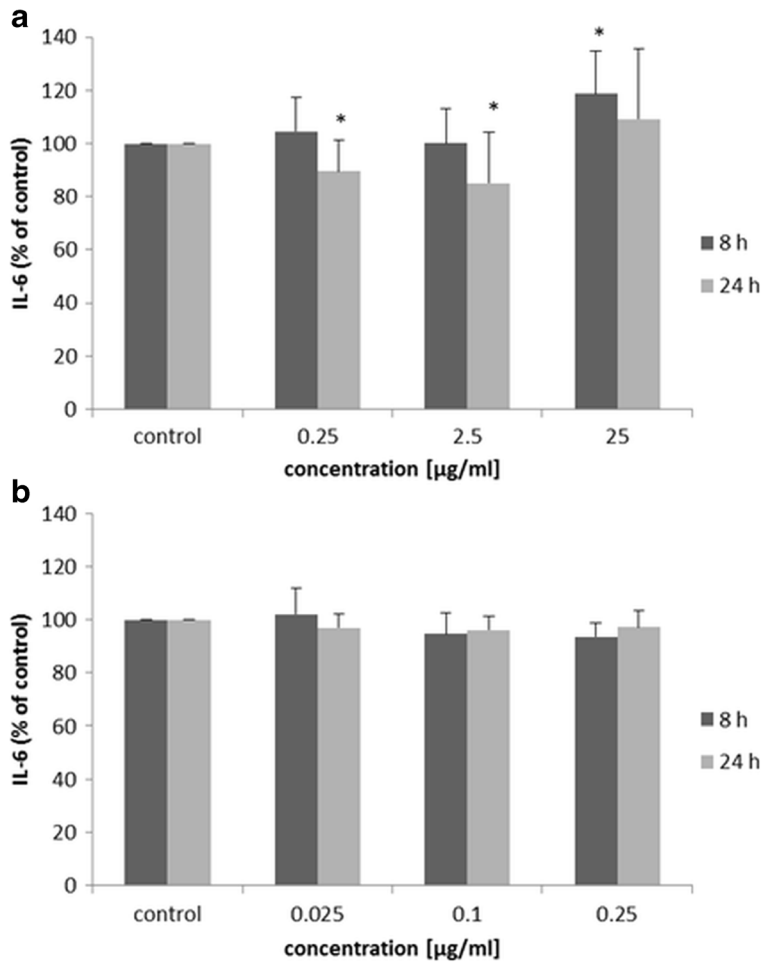

Fig. 8 Effects of AgNPs and Ag-I on IL-6 level in NHDF. Scratched and heated cells were treated with **a** AgNPs (0.25, 2.5, and 25 μg/ml) and **b** Ag-I (0.025, 0.1, and 0.25 μg/ml) for 8 and 24 h. Scratched and heated controls were treated with medium without AgNPs or Ag-I under the same conditions. The level of IL-6 in supernatants was determined by ELISA analysis. Data are representative of six independent experiments expressed as means + SD. $^*p \leq 0.05$ is significantly different from scratched and heated cells

serious morphological changes were observed by Kang et al. in an SKOV3 ovarial tumor cell line after 24 h of exposure to AgNPs (10 μg/ml) of diameter 7.5 ± 2.5 nm (Kang et al. 2012b). The differences between our results and the results of the above studies could be caused by the different cell types or by the nanoparticle concentration and size used in the individual studies.

Several studies have indicated that AgNPs are capable of producing ROS that in biological systems lead to oxidative stress. Carlson et al. reported a 10-fold increase in ROS level in alveolar macrophages exposed to AgNPs (50 μg/ml; 15 nm size) (Carlson et al. 2008). Increased ROS level was also observed in knockdown HK-2 cells exposed to AgNPs (60 μg/ml; 7.5 nm size) (Kang et al. 2012a), in normal human lung fibroblasts treated with AgNPs (25 and 50 μg/ml; 6–20 nm size) (Asha Rani et al. 2008), and in mouse skin cells exposed to AgNPs (100 μg/ml; 100–500 nm size) (Jebali and Kazemi 2013). Kaur et al. showed that AgNPs (50 μg/ml; 30–50 nm size) increased the ROS level in an A431 cell line but not in RAW macrophages, even at 100 μg/ml, due to the aggregation of AgNPs at the higher concentration. They further reported that RAW cells engulf AgNPs and thus resist any toxic response, whereas A431 cells have no such mechanism to prevent the toxicity of AgNPs (Kaur and Tikoo 2013). On the other hand, Ahlberg et al. found that AgNPs (10–50 μg/ml; 70 ± 20 nm size) decreased the ROS level in human keratinocytes after 3 h (Ahlberg et al. 2014). Our results showed that non-toxic concentrations of AgNPs (0.25, 2.5, and 25 μg/ml; 10.43 ± 4.74 nm) and Ag-I (0.025, 0.1, and 0.25 μg/ml) did not increase the ROS level in NHDF compared to untreated cells after 8 and 24 h (data not shown). These findings suggest that the ROS production induced by AgNPs strongly depends on the cell model and on the nanoparticle concentration and size.

Activated granulocyte neutrophils and macrophages in the wound produce a large amount of ROS (Keller et al. 2006) that decreased the fibroblast migration speed (Mamalis et al. 2015). The scratching and heating of NHDF provided a better approximation of our cell model to the reality. When ROS production is increased above the normal level, Nrf2 activates the expression of an array of antioxidant genes and stress-response proteins such as HO-1, resulting in the protection of cells against oxidative insults. AgNPs applied to the scratched and heated cells at the lower concentrations (0.25, 2.5 μg/ml) did not change the ROS level, but the concentration of 25 μg/ml non-significantly increased the ROS level after 8 h (Fig. 4a). Moreover, lower concentrations of AgNPs (0.25, 2.5 μg/ml) decreased the wound area after 24 and 48 h (Fig. 3a). These results correlated with the findings for nuclear Nrf2 level and HO-1 expression. We observed that lower concentrations of AgNPs (0.25 and 2.5 μg/ml) increased the nuclear Nrf2 level (Fig. 5a) and HO-1 expression (Fig. 6a) while 25 μg/ml decreased the nuclear Nrf2 level after 8 h. These results suggest that lower concentrations of AgNPs (0.25 and 2.5 μg/ml) protected the NHDF against oxidative stress and thus could improve wound healing through activation of the Nrf2 pathway. On the other hand, a higher concentration of AgNPs (25 μg/ml) suppresses the Nrf2 pathway and thus could increase the susceptibility of cells to oxidative stress and therefore could inhibit wound healing. These results must be verified at the gene level. However, the level of Nrf2 and the ROS generation in NHDF exposed to AgNPs (25 μg/ml) for 24 h contradicts this theory. This significant decrease in ROS could not be due to the Nrf2 activation of HO-1 expression. There is a possibility that higher concentrations of AgNPs can activate HO-1 expression and thus cause a decrease in ROS through another pathway stimulating redox-sensitive transcription factors, such as activating protein (AP-1) or heat shock factors (Alam and Cook 2007). There are confirmed reports that AgNPs can upregulate AP-1 (El-Ansary and Al-Daihan 2009). Further, we observed that AgNPs decreased the nuclear Nrf2 level and non-significantly increased the HO-1 expression in a concentration-dependent manner after 24 h. These results could be linked to the fact that the increases in Nrf2 and HO-1 level peaked 8 h after AgNP exposure and then subsequently declined 24 h after exposure. These observations are in agreement with the study of Aueviriyavit et al. (2014). When we compared AgNPs and Ag-I, surprisingly Ag-I at lower concentrations (0.025 and 0.1 μg/ml) increased the Nrf2 level more (Fig. 5b). Nevertheless, if we compare ROS generation (Fig. 4b), we do not observe as big a reduction for Ag-I as for AgNPs. The probable reason for this could be in the expression of HO-1 (Fig. 6b), because Ag-I caused a far lower increase in HO-1 than AgNPs. Previously, a few studies were focused on evaluating the effect of AgNPs on the Nrf2/HO-1 signaling pathway. Nevertheless, the results of the studies are contradictory. Kang et al. demonstrated an activation of the Nrf2/HO-1 signaling pathway in response to AgNPs (10 μg/ml) after 24 h of exposure in SK-OV3 cells (Kang et al. 2012b); similarly, Aueviriyavit et al. reported that AgNPs (15 and 40 μg/ml) activated the Nrf2/HO-1 signaling pathway in Caco-2 cells after 6 h of treatment (Aueviriyavit et al. 2014). On the other hand, Piao et al. showed that AgNPs (4 μg/ml) during 6–24 h of treatment decreased the nuclear Nrf2 expression, translocation into the nucleus, and transcriptional activity of Nrf2 in human Chang liver cells (Piao et al. 2011b). Taken together, the results of the above-mentioned studies suggest that the concentration of AgNPs above 10 μg/ml caused toxicity through the induction of ROS generation and the Nrf2/HO-1 signaling pathway plays an important role in the cytoprotective response to AgNP exposure in cells. On the other hand, the results of our study suggest that a lower concentration of AgNPs (0.25, 2.5 μg/ml) did not induce ROS generation, but could help to activate the Nrf2/HO-1 signaling pathway in the wound healing model and thus protect cells against oxidative stress and support wound healing (as shown in Fig. 3a).

Oxidative stress-induced redox signaling is known to involve the activation of transcription factors such as NF-κB which in turn induce the expression of various pro-inflammatory genes, including IL-6. This transcriptional factor is necessary for the immune response against invading microorganisms after wounds (Bonizzi and Karin 2004), but the prolonged overexpression of them can lead to chronic inflammation (Ben-Neriah and Karin 2011). Also, evaluating IL-6 during wound healing is very complicated. Its deficiency leads to bad skin healing and a long overexpression can cause scar formation (Liechty et al. 2000). Several recent studies have shown that AgNPs affect the NF-κB signaling pathway, but the results of these studies are contradictory. Some studies showed that AgNPs increased NF-κB expression (Asha Rani et al. 2012;

Table 2 Summary of our and previous published data for the effect of AgNPs on NF-κB expression

NF-κB expression	Concentration (μg/ml)	Size (nm)	Cell type	Incubation time (h)	Inventor
Increase	0.3, 1, 3	66.2–77.2	HepG2	24	(Prasad et al. 2013)
Increase	3, 10, 30	119–170	HepG2	24	(Prasad et al. 2013)
Increase	100	20 and 200	HepG2	6	(Stępkowski et al. 2014)
Increase	5	15, 25, 40 and 45	Mouse macrophages	24	(Nishanth et al. 2011)
Increase	20	140	NHDF	8 and 24	(Romoser et al. 2012)
Increase	0.05–0.2	5–10	Human T cells	24	(Eom and Choi 2010)
Increase	400	6–20	Lung and brain cells	48	(Asha Rani et al. 2012)
Did not change	100	20 and 200	Epithelial cells A549	6	(Stępkowski et al. 2014)
Decrease	50, 100, 150, 200	20–100	HCT116 colon cancer cells	48	(Satapathy et al. 2013)
Increase	0.25	10	NHDF	8	Our data
Decrease	0.25, 2.5	10	NHDF	24	Our data
Did not change	25	10	NHDF	8 and 24	Our data

Eom and Choi 2010; Nishanth et al. 2011; Prasad et al. 2013; Romoser et al. 2012; Stępkowski et al. 2014), resulting in the transcription of many genes involved in inflammatory response such as IL-6, IL-8, COX-2, and TNF-α (Eom and Choi 2010; Nishanth et al. 2011), but other studies reported that AgNPs did not change (Stępkowski et al. 2014) or decreased (Satapathy et al. 2013) NF-κB expression in cells (see Table 2). Similarly, the results in terms of the effects of AgNPs on IL-6 level are different. Samberg et al. reported an increased IL-6 level in human epidermal keratinocytes exposed to AgNPs (0.34 μg/ml; 20, 50, and 80 nm diameter) for 24 h (Samberg et al. 2010), while Greulich et al. found a decreased IL-6 level in human mesenchymal stem cells exposed to AgNPs (2.5 and 50 μg/ml; 100 nm size) as well as Ag-I (2.5 and 50 μg/ml) for 7 days (Greulich et al. 2009). Moreover, Yen et al. did not observe any effect of AgNPs (1 μg/ml; 2–40 nm size) on IL-6 level in macrophages (Yen et al. 2009). The results of our study showed that AgNPs (0.25 μg/ml; Fig. 7a) increased the NF-κB level in NHDF after 8 h, while a decrease in the NF-κB level in cells exposed to AgNPs (0.25 and 2.5 μg/ml) was observed after 24 h. These findings correspond with the IL-6 level. We found that AgNPs (0.25 and 2.5 μg/ml; Fig. 8a) decreased the IL-6 level in NHDF after 24 h. When we compared AgNPs with Ag-I, we did not find any trends. The results showed that Ag-I at a concentration of 0.1 μg/ml (Fig. 7b) increased the NF-κB level in NHDF after 8 h, while a decrease in NF-κB level in cells exposed to Ag-I (0.025 and 0.25 μg/ml) was observed after 24 h. Further, Ag-I (Fig. 8b) did not change the IL-6 level after 8 and 24 h. These results suggest that AgNPs (0.25 and 2.5 μg/ml) could prevent the formation of a chronic wound through suppression of the NF-κB pathway, but also these results must be verified at the gene level. Taken together, the results of the above-mentioned studies and our results suggest that the cell model, duration of exposure, and nanoparticle concentration and size seem to play a vital role in the involvement of AgNPs in NF-κB activation/inhibition.

In conclusion, non-cytotoxic concentrations of AgNPs (0.25 and 2.5 μg/ml) did not affect the ROS generation, but activated the Nrf2/HO-1 pathway and decreased the NF-κB and IL-6 protein levels in the in vitro wound healing model. Accordingly, AgNPs are suitable for the intended application as a topical agent for wound healing at concentrations of 0.25 and 2.5 μg/ml. Still, the gene silencing technique, chemical inhibitors, and detailed time- and concentration-dependent experiments are needed for a comprehensive study of signaling pathway regulation. Further investigation is also necessary to exclude any possible adverse effects after longer or regularly exposure, such as a safety evaluation after the topical application and skin absorption of AgNPs using human skin explants.

Acknowledgements We would like to thank Dr. Alena Rajnochová for a critical review of the manuscript. This work was supported by the grants from Palacký University (IGA_

LF_2015_007 and IGA_LF_2016_012), from the Ministry of Health of the Czech Republic (IGA 15-27726A), and by the National Programme for Sustainability I (L01304).

Compliance with ethical standards

Conflict of interest The authors declare that they have no conflicts of interest.

References

Ahlberg S et al (2014) Comparison of silver nanoparticles stored under air or argon with respect to the induction of intracellular free radicals and toxic effects toward keratinocytes. Eur J Pharm Biopharm 88:651–657

Alam J, Cook JL (2007) How many transcription factors does it take to turn on the heme oxygenase-1 gene? Am J Respir Cell Mol Biol 36:166–174

Alexander JW (2009) History of the medical use of silver. Surg Infect 10:289–292

Asha Rani PV, Low Kah Mun G, Hande MP, Valiyaveettil S (2008) Cytotoxicity and genotoxicity of silver nanoparticles in human cells. ACS Nano 3:279–290

Asha Rani P, Sethu S, Lim HK, Balaji G, Valiyaveettil S, Hande MP (2012) Differential regulation of intracellular factors mediating cell cycle, DNA repair and inflammation following exposure to silver nanoparticles in human cells. Genome Integr 3:2

Aueviriyavit S, Phummiratch D, Maniratanachote R (2014) Mechanistic study on the biological effects of silver and gold nanoparticles in Caco-2 cells–induction of the Nrf2/HO-1 pathway by high concentrations of silver nanoparticles. Toxicol Lett 224:73–83

Ben-Neriah Y, Karin M (2011) Inflammation meets cancer, with NF-kappa B as the matchmaker. Nat Immunol 12:715–723. doi:10.1038/Ni.2060

Bonizzi G, Karin M (2004) The two NF-kappa B activation pathways and their role in innate and adaptive immunity. Trends Immunol 25:280–288. doi:10.1016/J.It.2004.03.008

Carlson C, Hussain S, Schrand A, Braydich-Stolle LK, Hess K, Jones R, Schlager J (2008) Unique cellular interaction of silver nanoparticles: size-dependent generation of reactive oxygen species. J Phys Chem B 112:13608–13619

El-Ansary A, Al-Daihan S (2009) On the toxicity of therapeutically used nanoparticles: an overview. J Toxicol 2009: 754810

Eom H-J, Choi J (2010) p38 MAPK activation, DNA damage, cell cycle arrest and apoptosis as mechanisms of toxicity of silver nanoparticles in Jurkat T cells. Environ Sci Technol 44:8337–8342

Galandáková A et al (2016) Effects of silver nanoparticles on human dermal fibroblasts and epidermal keratinocytes. Hum Exp Toxicol 35:946–957. doi:10.1177/0960327115611969

Ghosh S, May MJ, Kopp EB (1998) NF-kappa B and rel proteins: evolutionarily conserved mediators of immune responses. Annu Rev Immunol 16:225–260. doi:10.1146/annurev.immunol.16.1.225

Greulich C, Kittler S, Epple M, Muhr G, Köller M (2009) Studies on the biocompatibility and the interaction of silver nanoparticles with human mesenchymal stem cells (hMSCs). Langenbeck's Arch Surg 394:495–502

Jebali A, Kazemi B (2013) Triglyceride-coated nanoparticles: skin toxicity and effect of UV/IR irradiation on them. Toxicol in Vitro 27:1847–1854

Kang SJ, Lee YJ, Lee E-K, Kwak M-K (2012a) Silver nanoparticles-mediated G2/M cycle arrest of renal epithelial cells is associated with NRF2-GSH signaling. Toxicol Lett 211:334–341

Kang SJ, Ryoo I-G, Lee YJ, Kwak M-K (2012b) Role of the Nrf2-heme oxygenase-1 pathway in silver nanoparticle-mediated cytotoxicity. Toxicol Appl Pharmacol 258:89–98

Kaur J, Tikoo K (2013) Evaluating cell specific cytotoxicity of differentially charged silver nanoparticles. Food Chem Toxicol 51:1–14

Keller UAD et al (2006) Nrf transcription factors in keratinocytes are essential for skin tumor prevention but not for wound healing. Mol Cell Biol 26:3773–3784. doi:10.1128/Mcb.26.10.3773-3784.2006

Kvítek L, Panáček A, Prucek R (2013) Process for preparing aqueous dispersions of metal nanoparticles

Kwan KH, Liu X, To MK, Yeung KW, Ho CM, Wong KK (2011) Modulation of collagen alignment by silver nanoparticles results in better mechanical properties in wound healing. Nanomedicine 7:497–504

Lee Y-H, Cheng F-Y, Chiu H-W, Tsai J-C, Fang C-Y, Chen C-W, Wang Y-J (2014) Cytotoxicity, oxidative stress, apoptosis and the autophagic effects of silver nanoparticles in mouse embryonic fibroblasts. Biomaterials 35:4706–4715

Liang C-C, Park AY, Guan J-L (2007) In vitro scratch assay: a convenient and inexpensive method for analysis of cell migration in vitro. Nat Protoc 2:329–333

Liechty KW, Adzick NS, Crombleholme TM (2000) Diminished interleukin 6 (IL-6) production during scarless human fetal wound repair. Cytokine 12:671–676

Liu X et al (2010) Silver nanoparticles mediate differential responses in keratinocytes and fibroblasts during skin wound healing. Chem Med Chem 5:468–475

Mamalis A et al (2015) Resveratrol prevents high fluence red light-emitting diode reactive oxygen species-mediated photoinhibition of human skin fibroblast migration. PLoS One 10:1–9. doi:10.1371/journal.pone.0140628

Negre-Salvayre A et al (2002) [5] Detection of intracellular reactive oxygen species in cultured cells using fluorescent probes. Methods Enzymol 352:62–71

Nishanth RP, Jyotsna RG, Schlager JJ, Hussain SM, Reddanna P (2011) Inflammatory responses of RAW 264.7 macrophages upon exposure to nanoparticles: role of ROS-NFκB signaling pathway. Nanotoxicology 5:502–516

Pedersen TX et al (2003) Laser capture microdissection-based in vivo genomic profiling of wound keratinocytes identifies similarities and differences to squamous cell carcinoma. Oncogene 22:3964–3976. doi:10.1038/sj.onc.1206614

Piao MJ et al (2011a) Silver nanoparticles induce oxidative cell damage in human liver cells through inhibition of reduced glutathione and induction of mitochondria-involved apoptosis. Toxicol Lett 201:92–100

Piao MJ, Kim KC, Choi J-Y, Choi J, Hyun JW (2011b) Silver nanoparticles down-regulate Nrf2-mediated 8-oxoguanine DNA glycosylase 1 through inactivation of extracellular regulated kinase and protein kinase B in human Chang liver cells. Toxicol Lett 207:143–148

Prasad RY, McGee JK, Killius MG, Suarez DA, Blackman CF, DeMarini DM, Simmons SO (2013) Investigating oxidative stress and inflammatory responses elicited by silver nanoparticles using high-throughput reporter genes in HepG2 cells: effect of size, surface coating, and intracellular uptake. Toxicol in Vitro 27:2013–2021

Romoser AA et al (2012) Distinct immunomodulatory effects of a panel of nanomaterials in human dermal fibroblasts. Toxicol Lett 210:293–301

Samberg ME, Oldenburg SJ, Monteiro-Riviere NA (2010) Evaluation of silver nanoparticle toxicity in skin in vivo and keratinocytes in vitro. Environ Health Perspect 118:407–413

Satapathy SR et al (2013) Silver-based nanoparticles induce apoptosis in human colon cancer cells mediated through p53. Nanomedicine (Lond) 8:1307–1322

Stępkowski T, Brzóska K, Kruszewski M (2014) Silver nanoparticles induced changes in the expression of NF-κB related genes are cell type specific and related to the basal activity of NF-κB. Toxicol in Vitro 28:473–478

Tian J et al (2007) Topical delivery of silver nanoparticles promotes wound healing. Chem Med Chem 2:129–136

Yen HJ, Hsu S, Tsai CL (2009) Cytotoxicity and immunological response of gold and silver nanoparticles of different sizes. Small 5:1553–1561